



 Cite this: *RSC Adv.*, 2020, 10, 21852

# Preparation of quercetin–nicotinamide cocrystals and their evaluation under *in vivo* and *in vitro* conditions†

 Na Wu,<sup>ab</sup> Yan Zhang,<sup>b</sup> Jian Ren,<sup>b</sup> Aiguo Zeng<sup>c</sup> and Juntian Liu <sup>\*a</sup>

Quercetin is a flavonoid abundant in the plant kingdom. Various types of bioactivities of quercetin have been demonstrated *in vitro*. Although quercetin has been proposed to exhibit numerous pharmacological benefits, it suffers from low bioavailability on account of its obviously poor solubility in water. Cocrystals have generated interest recently as a way of enhancing the dissolution *in vitro* and creating relative bioavailability of insoluble medicine. In this study, quercetin–nicotinamide cocrystals were obtained via a solvent evaporation technique. Furthermore, quercetin–nicotinamide cocrystals were characterized via Fourier transform infrared (FT-IR) spectroscopy, X-ray powder diffraction (PXRD), and differential scanning calorimetry (DSC) techniques. Quercetin–nicotinamide cocrystals are a new phase material, and the established intermolecular forces such as hydrogen bonds between quercetin and nicotinamide existed in the quercetin–nicotinamide cocrystals, as confirmed from the solid-state analysis. The dissolution of quercetin–nicotinamide cocrystals was found to be significantly higher than that of quercetin crystals. The pharmacokinetic data from the *in vivo* experiments suggested that quercetin–nicotinamide cocrystals could significantly increase the oral absorption of quercetin by nearly 4-fold. These results demonstrate that the developed quercetin–nicotinamide cocrystals are a promising oral formulation toward improvement in the dissolution and bioavailability of quercetin.

 Received 14th April 2020  
 Accepted 12th May 2020

DOI: 10.1039/d0ra03324c

[rsc.li/rsc-advances](http://rsc.li/rsc-advances)

## 1 Introduction

Flavonoids exist extensively in nature, and some of these compounds possess medicinal value, such as antioxidant, free radical scavenging and antitumor activities.<sup>1</sup> Numerous studies have shown protective effects of flavonoids against cardiovascular diseases and senility through antioxidant-free radical activity, and tumor by reducing drug resistance, and so on.<sup>2</sup> Quercetin (3,3',4',5,7-pentahydroxyflavone), a naturally occurring biological flavonoid, mainly comes from acerola cherries, tea, red onions, raspberries, blueberries and other plants and displays a strong antioxidant activity<sup>3</sup> and other bioactivities including anti-inflammatory, anti-tumor, cardioprotective and metal chelating effects.<sup>4–7</sup>

Although quercetin has numerous beneficial effects on humans, its extremely low solubility in water limits its development and applications. It is reported that the oral absorption

of quercetin in the gastrointestinal system is very low, only 2%,<sup>8–10</sup> due to its high crystallinity that causes the low absorption of quercetin. Therefore, the improvement of quercetin solubility in water is necessary to increase its bioavailability.

For the past few years, some techniques have been applied to increase the dissolution and bioavailability of quercetin, such as amorphous solid dispersion, nanoencapsulation, and cocrystallization.<sup>11–13</sup> Cocrystals are multi-component crystalline systems composed of different molecular and/or ionic compounds with some order in the proportion. However, the solid is neither a simple solvent complex nor a salt.<sup>14,15</sup> In recent years, scientists have changed the physicochemical properties of solids, such as the dissolution, stability, physicochemical properties, bioavailability and mechanical properties using cocrystals and without affecting the activity of the original insoluble solid medicine.<sup>16,17</sup> Cocrystals with active pharmaceutical ingredient (API) and different excipients, or of different stoichiometry with the same cocrystals as that of former, have a different crystal structure and bring about different physicochemical properties.<sup>18,19</sup> The cocrystals of quercetin with caffeine or isonicotinamide/theobromine formed by hydrogen bonds can improve the water solubility of quercetin, and increase the bioavailability of quercetin by up to 10 folds.<sup>20</sup>

In this experiment, nicotinamide was chosen as a cocrystal former, and cocrystals of quercetin–nicotinamide with different stoichiometries were prepared. Furthermore, we characterized

<sup>a</sup>School of Basic Medical Sciences, Health Science Center, Xi'an Jiaotong University, 76 West Yanta Road, Xi'an, 710061, China. E-mail: [ljt@mail.xjtu.edu.cn](mailto:ljt@mail.xjtu.edu.cn); Tel: +86-29-82665188

<sup>b</sup>The Eighth Hospital of Xi'an, 2 East Zhangba Street, Xi'an, 710061, China

<sup>c</sup>School of Pharmacy, Health Science Center, Xi'an Jiaotong University, 76 West Yanta Road, Xi'an, 710061, China

† Electronic supplementary information (ESI) available. See DOI: 10.1039/d0ra03324c



the cocrystals by numerous analytic methods and investigated their dissolution and bioavailability.

## 2 Experiments and methods

Quercetin (98% purity) and nicotinamide (99% purity) were purchased from Xi'an Shuaidi Biotechnology Co., Ltd (Xi'an, Shaanxi, China). Methanol, acetonitrile and all other chemical reagents were obtained from Guangdong Chemical Reagent Engineering Enterprise R&D Centers of Chromatographical Pure (Guangzhou, Guangdong, China). An Agilent C18 column and an AT-130 column oven (150 × 4.6 mm, 5 μm) used in the experiment were purchased from Hangzhou Ruixi Technology Co., Ltd (Hangzhou, Zhejiang, China).

Sprague-Dawley (SD) rats, weighing 240 to 290 g, were provided by Laboratory Animal Center of Health Science Center of Xi'an Jiaotong University (Xi'an, Shaanxi, China), and the experiments were approved with the standards of ethical review. All of the experimental protocols involving animals were reviewed and approved by the Medical Ethics Committee of the Xi'an Jiaotong University of Chinese Medicine Animal Care. 'Principles of Laboratory Animal Care' (NIH) and Guidelines of the Laboratory Animal Care Committee of Xi'an Jiaotong University were obeyed.

### 2.1 Preparation of quercetin–nicotinamide cocrystals

Quercetin and nicotinamide in the molar mass ratios of 1 : 1 (302.0 mg quercetin with 122.0 mg nicotinamide) and 1 : 2 (302.0 mg quercetin with 244.0 mg nicotinamide) were dissolved in 25 mL absolute ethanol at 80 °C and filtered using a filter paper. The filtrate was slowly evaporated at room temperature to harvest the yellow crystals of the two cocrystals.

### 2.2 Analysis *via* powder X-ray diffraction (PXRD)

PXRD measurements were performed using a Bruker D8 ADVANCE instrument with Cu K $\alpha$  radiation and operating at 2000 W with 30 mA and 40 kV, respectively. All samples were measured in the 2 $\theta$  range of 5–45° at a step interval of 0.02°. The Jade software (version 6.5) was used to analyze the measurement data in this study.

### 2.3 Differential scanning calorimetry (DSC)

The DSC thermograms were obtained using a DSC 822<sup>e</sup> (METTLER TOLEDO, Switzerland) instrument. All samples were loaded in aluminum pans, and the instrument was calibrated by an indium standard. An empty pan and samples were sealed and used for comparative testing. Samples were heated from 25 °C to 350 °C at a heating rate of 10 °C min<sup>-1</sup> in an inert nitrogen atmosphere. We performed data analysis using STAR<sup>e</sup> software (version 10.00). The STAR<sup>e</sup> software (version 10.00) was employed to analyze the DSC results.

### 2.4 Infrared spectroscopy (FT-IR)

A Shimadzu FT-IR 8400S system (Shimadzu, Japan) was employed to record the FT-IR spectra in the range of 4000 to

400 cm<sup>-1</sup> (15 scans per spectrum). Samples were fully ground, followed by the addition of an appropriate amount of KBr powder and continue grinding until the particle size was less than 2 μm. Samples were placed in the mold and pressed into a transparent wafer before recording their IR spectra. The IR solution software was used to analyze the FT-IR results.

### 2.5 Dissolution test

The dissolution test of quercetin (70 mg) and quercetin–nicotinamide cocrystals (equivalent to 70 mg quercetin) was performed using the ZRS-8LD intelligent dissolution tester (Tianjin Tianda Tianfa Technology Co. Ltd, China), using 200 mL water as a dissolution medium at the temperature of 37.5 ± 0.5 °C and at the velocity of rotation of 100 rpm. The *in vitro* dissolution of quercetin was performed by a slurry method for 6 h at the sampling time of 5, 10, 15, 20, 30, 60, 120, 180, 240, 300 and 360 min, and the samples were passed through a 0.45 μm microporous membrane filter. At a given sampling time, volume and temperature of the fresh dissolution medium were adjusted to correct the cumulative dilution. The sample concentrations were determined *via* high-performance liquid chromatography (HPLC) after filtration and dilution. All dissolution experiments were performed in triplicates.

The chromatographic separation was obtained with a moving phase made up of methanol and 0.1% phosphoric acid (55 : 45, bulk factor). Moreover, the flow rate of the moving phase was controlled at 1.0 mL min<sup>-1</sup>. The oven used for the chromatographic column was controlled at 30 °C. All the samples were analyzed *via* HPLC on a UV detector at 254 nm.

### 2.6 Pharmacokinetics in rats

SD rats used in this study were fed an absolute diet (water for free) for 12 h continuously before the experiment. 10 male SD rats were stochastically divided into two groups for the oral administration of a bolus dose of quercetin or quercetin–nicotinamide cocrystals (1 : 1), respectively. The suspensions of quercetin (10 mg kg<sup>-1</sup>) were composed of 2 mL 0.5% CMC-Na and quercetin, and quercetin–nicotinamide cocrystals (1 : 1) equivalent to quercetin level of 10 mg kg<sup>-1</sup>. The blood samples were collected from the jugular vein at 0, 5, 10, 30, 60, 120, 240, 360, 480 and 720 min in heparinized tubes. Then, the blood samples were centrifuged for ten min (3000 rpm) and the obtained plasma samples were refrigerated at –80 °C for testing.

The liquid–liquid extraction technique was used in plasma samples. Briefly, for a 0.5 μg mL<sup>-1</sup> sample, 50 μL of genistein (internal standard) solution was added into the centrifuge tube and volatilized to dryness. 200 μL of the plasma samples were accurately measured, put into a centrifuge tube with the internal standard for volatile drying, then 0.5 mL of ethyl acetate was added, swirled blended for 1 min, and centrifuged (3500 rpm, 5 min). After standing for a while, the upper layer was transferred into another clean test tube, blow-dried under a nitrogen flow. The remaining obtained residue was redissolved in 50 μL of methanol, swirled for 1 min, and centrifuged (12 000 rpm, 5 min); after standing for a while, 20 μL of the



supernatant liquid was injected into the HPLC system, and the analysis results were recorded.

The chromatographic separation was obtained with a moving phase, comprising acetonitrile, methanol and 0.1% phosphoric acid (30 : 5 : 65, bulk factor), and under a controlled flow velocity of 1.0 mL min<sup>-1</sup>. The oven was maintained at 30 °C. The ratio of the chromatographic peak area of quercetin to an internal standard by UV absorbency at 254 nm was determined for quantitative analysis.

The WinNolin software (version 5.2) was used to match the non-compartment model of the measured pharmacokinetic

data and the Student's *t*-test was used for the statistical analysis. The SPSS software (version 18) was employed for the statistical analysis ( $p < 0.05$ ).

### 3 Results and discussion

#### 3.1 Solid state characterization

**PXRD.** The PXRD data is shown in Fig. 1. Quercetin had strong crystal characteristic diffraction peaks at  $2\theta = 8.84^\circ$ ,  $16.54^\circ$  and  $27.42^\circ$ . The characteristic diffraction peaks of the physical mixture of quercetin and nicotinamide are equivalent

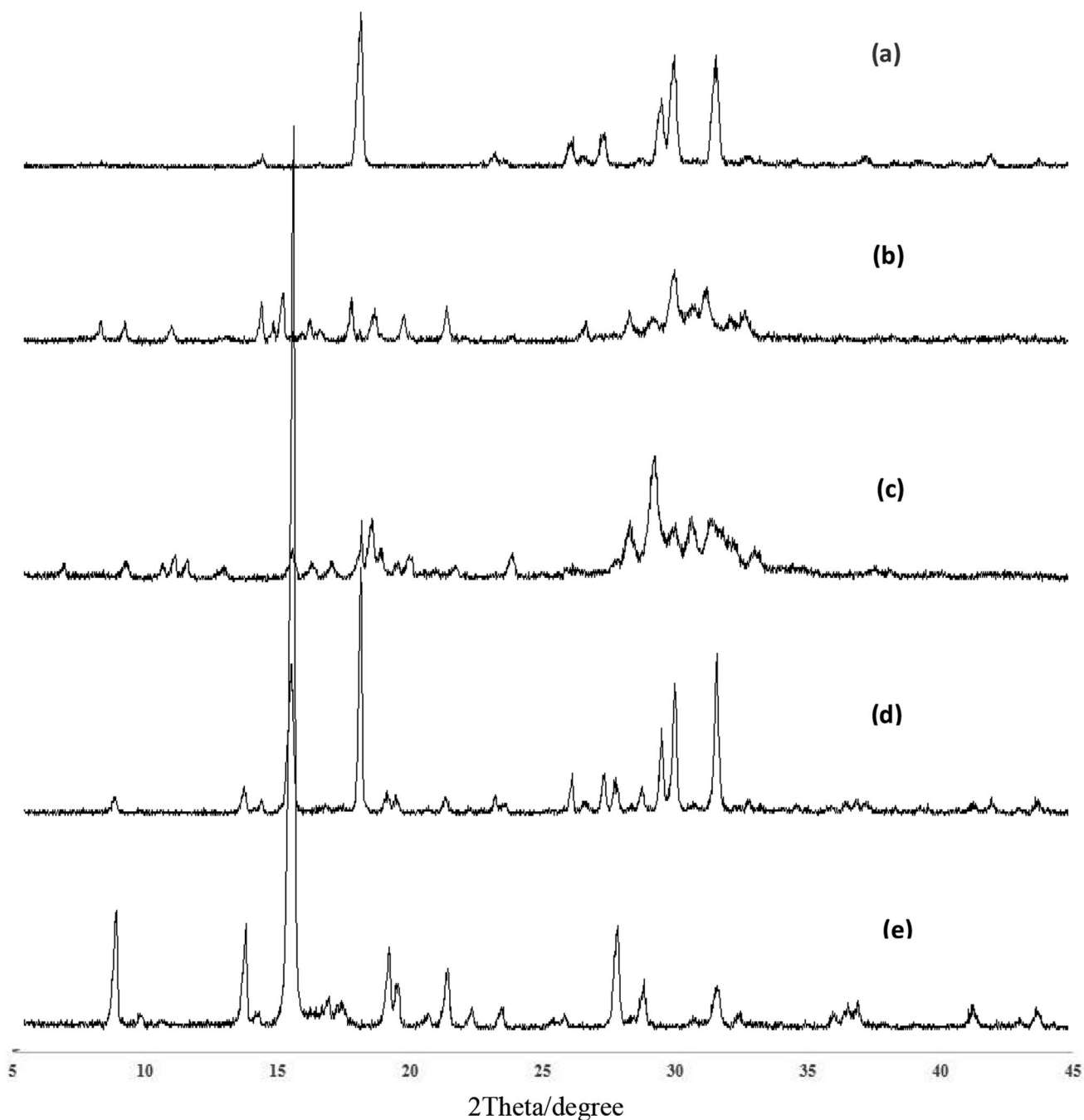


Fig. 1 PXRD patterns of nicotinamide, quercetin–nicotinamide cocrystals (1 : 1 and 1 : 2), physical mixture (1 : 1) and quercetin (up to bottom); (a) nicotinamide, (b) quercetin–nicotinamide cocrystal (1 : 1), (c) quercetin–nicotinamide cocrystal (1 : 2), (d) physical mixture (1 : 1), (e) quercetin.



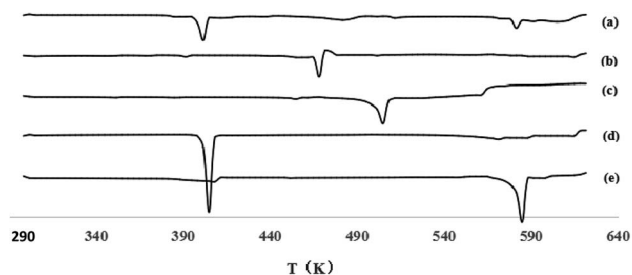


Fig. 2 DSC thermograms for nicotinamide, quercetin–nicotinamide cocrystals (1 : 1 and 1 : 2), physical mixture (1 : 1) and quercetin, (a) physical mixture (1 : 1), (b) quercetin–nicotinamide cocrystal (1 : 2), (c) quercetin–nicotinamide cocrystal (1 : 1), (d) nicotinamide, (e) quercetin.

to the superimposed peaks of quercetin and nicotinamide. Simultaneously, the characteristic diffraction peaks of quercetin–nicotinamide cocrystals (1 : 1 and 1 : 2) were different from the physical mixture of quercetin and nicotinamide. A new phase was formed as seen from the patterns.

**DSC.** DSC figures for the melting point are shown in Fig. 2. The melting point peaks of quercetin and nicotinamide are 313.43 °C and 131.77 °C, respectively. The curve for the physical mixture was equivalent to that of the superimposed quercetin and nicotinamide. The melting points of quercetin–nicotinamide cocrystals (1 : 1) and quercetin–nicotinamide cocrystals (1 : 2) were 231.77 °C and 195.1 °C, respectively. These results were different from the physical mixture of quercetin and nicotinamide. The formation of some new phases was also observed. The same conclusions were reached from the PXRD figures.

**FT-IR.** The FT-IR spectra were recorded to evaluate the intermolecular forces between quercetin and nicotinamide in quercetin–nicotinamide cocrystals. It is well known that the formation of non-covalent bonds such as hydrogen bonds often

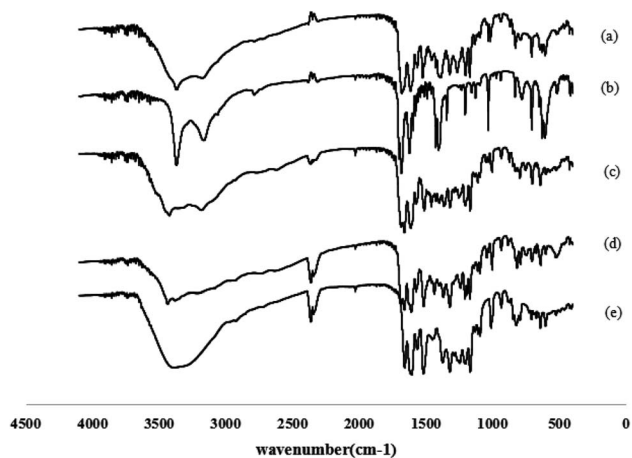


Fig. 3 FT-IR spectra showing the region from 4000  $\text{cm}^{-1}$  to 400  $\text{cm}^{-1}$  of quercetin, nicotinamide, physical mixture (1 : 1) and quercetin–nicotinamide cocrystals (1 : 1 and 1 : 2), (a) physical mixture (1 : 1); (b) nicotinamide; (c) quercetin–nicotinamide cocrystal (1 : 2), (d) quercetin–nicotinamide cocrystal (1 : 1); (e) quercetin.

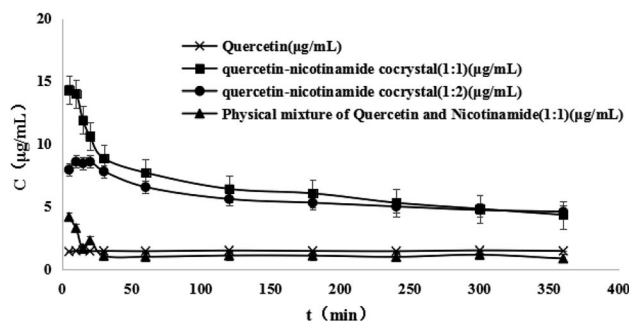


Fig. 4 Dissolution profiles of quercetin, physical mixture (1 : 1) and quercetin–nicotinamide cocrystals (1 : 1 and 1 : 2) in water.

leads to the shifting or broadening of the characteristic peaks corresponding to active pharmaceutical ingredients and different cocrystal formers in FT-IR spectra.<sup>21</sup>

The FT-IR spectra of quercetin, nicotinamide, physical mixture (1 : 1) and quercetin–nicotinamide cocrystals (1 : 1 and 1 : 2) are shown in Fig. 3. The characteristic peak for quercetin is observed at 3560  $\text{cm}^{-1}$  (O–H stretching vibrations), while the peak for quercetin–nicotinamide cocrystals (1 : 1) is at 3230  $\text{cm}^{-1}$ . The characteristic peaks for nicotinamide were generally seen at 1690  $\text{cm}^{-1}$  (C=O stretching vibrations) and 3520  $\text{cm}^{-1}$  (N–H stretching vibrations), but the enhanced characteristic peaks for quercetin–nicotinamide cocrystals (1 : 1) are observed at 1630  $\text{cm}^{-1}$  and 3350  $\text{cm}^{-1}$ . Comparing with quercetin and nicotinamide, the FT-IR spectra of quercetin–nicotinamide cocrystals show peak shifts (3560  $\rightarrow$  3230  $\text{cm}^{-1}$  for O–H stretching vibrations, 1690  $\rightarrow$  1630  $\text{cm}^{-1}$  for C=O vibrations, and 3520  $\rightarrow$  3350  $\text{cm}^{-1}$  for N–H stretching vibrations). This could be due to the formation of hydrogen bonds between quercetin and nicotinamide in quercetin–nicotinamide cocrystals, which might change some peak positions and shapes. The characteristic FT-IR absorption peaks for the physical mixture of quercetin and nicotinamide were the same as those of the superimposed peaks of quercetin and nicotinamide, which proved that the simple mixture of quercetin and nicotinamide had no interaction with each other. The physical mixture of quercetin and nicotinamide did not exhibit any intermolecular forces with each other. The same results are also seen in PXRD and DSC.

Table 1 The main pharmacokinetic data of quercetin and quercetin–nicotinamide cocrystals (1 : 1) in rats ( $n = 5$ )

Parameters	Unit	Quercetin	Quercetin–nicotinamide cocrystals
$t_{1/2}(k_p)$	min	1.06	1.97
$t_{1/2}(k_e)$	min	$4.96 \times 10^3$	$1.47 \times 10^4$
$T_{\text{max}}$	min	12.87	25.31
$C_{\text{max}}$	$\mu\text{g mL}^{-1}$	0.54	0.71
$\text{AUC}_{0-12}$	$(\mu\text{g mL}^{-1}) \times \text{min}$	$3.88 \times 10^3$	$1.52 \times 10^4$
$K_a$	$\text{min}^{-1}$	0.66	0.35
$K_e$	$\text{min}^{-1}$	$1.4 \times 10^{-4}$	$4.7 \times 10^{-5}$



### 3.2 Dissolution

The dissolution curves for quercetin, nicotinamide, physical mixture (1 : 1) and quercetin–nicotinamide cocrystals (1 : 1 and

1 : 2) in water are shown in Fig. 4. The *in vitro* dissolution of quercetin was determined by the slurry method, in the same way, it was for quercetin–nicotinamide cocrystals (1 : 1 and

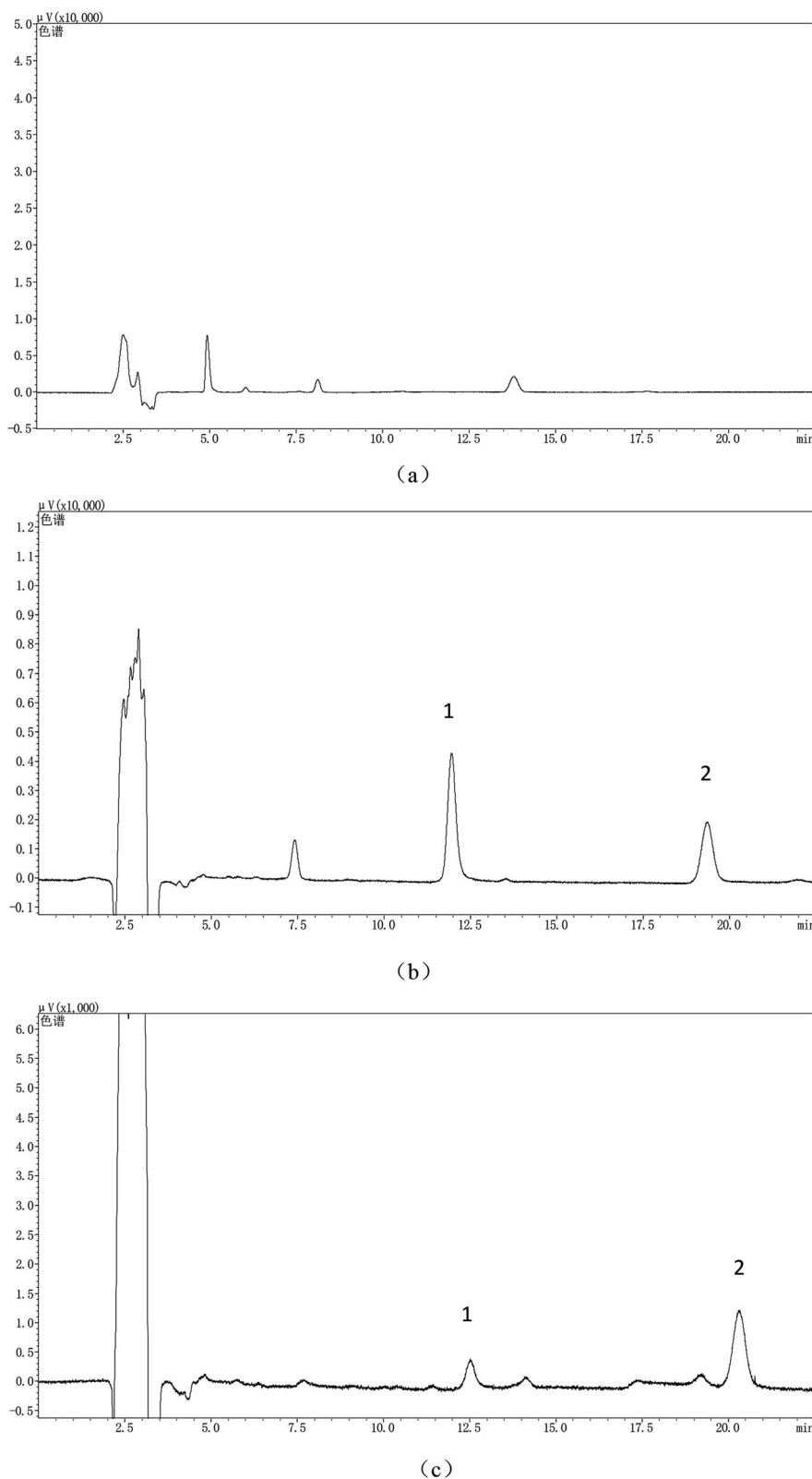


Fig. 5 HPLC chromatograms of blank rat plasma (a), rat plasma spiked with quercetin plus genistein (b) and rat plasma sample after the oral administration ( $10 \text{ mg kg}^{-1}$ ) of quercetin or quercetin–nicotinamide cocrystals (1 : 1) (c). (1), quercetin; (2), genistein.



1 : 2) and the physical mixture. In this study, pure water was used as a dissolution medium and the samples were taken for 6 h at 5, 10, 15, 20, 30, 60, 120, 180, 240, 300 and 360 min, respectively. The dissolution tester temperature was maintained at  $37.5 \pm 0.5$  °C. Quercetin had very poor water solubility, and the plateau concentration of quercetin was  $1.5 \mu\text{g mL}^{-1}$ , which agreed with reported by M. *et al.* ( $3 \mu\text{g mL}^{-1}$ ).<sup>22</sup> The dissolution curve of quercetin was similar to that of the physical mixture of quercetin and nicotinamide. However, quercetin–nicotinamide cocrystals (1 : 1 and 1 : 2) had better dissolution than the quercetin crystal in our study. It is important to note that quercetin–nicotinamide cocrystals (1 : 1 and 1 : 2) showed a significantly faster dissolution rate and supersaturated dissolution curve. Within 15 min, the dissolution rate of quercetin–nicotinamide cocrystals (1 : 1 and 1 : 2) was faster than that of quercetin. The peak concentration of quercetin–nicotinamide cocrystals (1 : 1 and 1 : 2) was 10 and 6 times the quercetin solubility, respectively. It was concluded that the rapid dissolution and higher solubility of quercetin–nicotinamide cocrystals were due to a strong hydrophilic effect. Quercetin was not easily dispersed in water and is highly hydrophobic. After reaching a peak concentration, the concentration of quercetin–nicotinamide cocrystals is gradually decreased and was  $4.5 \mu\text{g mL}^{-1}$  at 6 h and 3 times the quercetin solubility. The downdrift of concentration was due to the recrystallization of quercetin during the dissolution experiment. The drastic increase in the solubility and faster dissolution rate for quercetin–nicotinamide cocrystals could benefit the oral bioavailability of quercetin and help to develop various applications.

### 3.3 Pharmacokinetics

It is a hypothesis that the increase in dissolution could result in improving the bioavailability of quercetin–nicotinamide cocrystals. The bioavailability of quercetin–nicotinamide cocrystals was evaluated by pharmacokinetic parameters in rats. Quercetin–nicotinamide cocrystals (1 : 1) were chosen to evaluate the bioavailability of quercetin–nicotinamide cocrystals due to their highest supersaturated dissolution.

First, the methodology was verified *via* high performance liquid chromatography in this experiment. The experimental data showed that the peak values of quercetin and genistein (internal standard) were 12.4 min and 19.5 min, respectively, from high-performance liquid chromatography and two peaks were completely separated. The endogenous impurities in the plasma did not interfere with the determination of quercetin and genistein. The standard calibration curve, which consisted of six incremental sample concentrations ( $n = 3$ ) of quercetin was constructed from the ratio of peak area and indicated a linear relationship between quercetin and genistein as a functional relationship of quercetin in the calculation of the plasma concentrations ( $Y = 0.55X - 0.2682$ ), and showing favorable linearity relationship ( $r = 0.9990$ ) at the effective concentration range of 0.4 to  $8 \mu\text{g mL}^{-1}$ . The quantification limit ( $S/N = 10$ ) ( $S/N$ : signal-to-noise) and the detection limit ( $S/N = 3$ ) for high-performance liquid chromatography were 4 ng

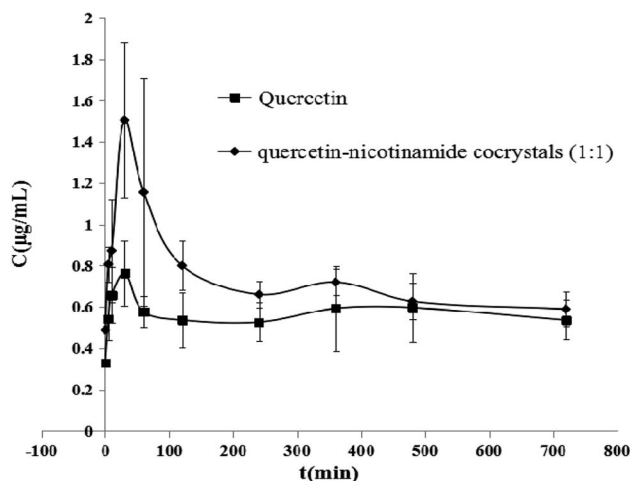


Fig. 6 Plasma concentration–time curves of quercetin in rats after the oral administration ( $10 \text{ mg kg}^{-1}$ ) of quercetin or quercetin–nicotinamide cocrystals (1 : 1) ( $n = 5$ ).

and 1 ng, respectively. The extraction recovery and method recovery for blank plasma samples matched the three different concentrations. The scope of the accuracy of quercetin was from 95% to 104%, and the intra-day to inter-day RSD ranged from 1.37% to 5.35%, respectively. In summary, the validation consequences of methodology suggested that the method of HPLC in this study was dependable and acceptable.

The pharmacokinetic curves after the oral administration ( $10 \text{ mg kg}^{-1}$ ) of quercetin and quercetin–nicotinamide cocrystals (1 : 1) to rats are exhibited in Fig. 6. The accurate data of pharmacokinetic parameters are exhibited in Table 1. As expected, the oral absorption of quercetin was very poor because of its poor solubility. However, the blood concentration of quercetin was obviously higher than that of the quercetin crystal after the oral administration of quercetin–nicotinamide cocrystals (1 : 1), containing the equivalent amount of quercetin. The maximum blood concentration ( $C_{\text{max}}$ ) was 1.3-fold superior to that of quercetin crystals, indicating that quercetin–nicotinamide cocrystals could enhance the absorption of oral quercetin. The area of quercetin under the curve ( $\text{AUC}_{0-12}$ ) obviously increased, and the relative bioavailability of quercetin was 392% in the quercetin–nicotinamide cocrystals (1 : 1). These results suggest that quercetin–nicotinamide cocrystals effectively enhance the oral bioavailability of quercetin (Fig. 5).

## 4 Discussion

PXRD, DSC and FT-IR are commonly used techniques for phase identifications. In this experiment, DSC is an analytic method to measure the change of enthalpy between the sample and the reference under the condition of the temperature range in a program, and the area of the curve is proportional to the change of enthalpy. An air atmosphere was used as a reference in this experiment. So, the data obtained are the enthalpy ratios of the samples, such as quercetin, quercetin–nicotinamide cocrystals (1 : 1 and 1 : 2) and the physical mixture of quercetin and nicotinamide. Different changes in enthalpy are



corresponding to the different phases. Quercetin–nicotinamide cocrystals (1 : 1 and 1 : 2) is a new phase obviously. Just the DSC is sometimes not able to accurately identify the presence of cocrystals and should be combined with other detection methods. As is known, the specific crystals have characteristic cell parameters and crystal structures. PXRD patterns show that quercetin–nicotinamide cocrystals (1 : 1 and 1 : 2) are new crystals different from quercetin crystals and their physical mixture. The FT-IR curves show that some hydrogen bonds are formed between quercetin and nicotinamide in quercetin–nicotinamide cocrystals.

The slurry method was used in this study to measure the dissolution of samples. Pure water was adopted as the dissolution medium. The dissolution of quercetin–nicotinamide cocrystals (1 : 1 and 1 : 2) was higher than that of quercetin crystals. In the *in vivo* experiments, HPLC was used to measure the plasma concentration of quercetin. We have initially established an appropriate analytical method of stabilization, accuracy, and sensitivity. The quercetin–nicotinamide cocrystals effectively increase the drug concentration of quercetin in rats. After fitting the data by software, the maximum blood concentration ( $C_{\max}$ ) of quercetin–nicotinamide cocrystals (1 : 1) was  $0.71 \mu\text{g mL}^{-1}$ , and the area under the curve (AUC) was  $15\,216.63 (\mu\text{g mL}^{-1})\cdot\text{min}$ . The drug concentration of insoluble drugs will be increased *in vivo* by the cocrystal method, and oral bioavailability will be improved.

## 5 Conclusion

In this study, we obtained quercetin–nicotinamide cocrystals *via* the solvent evaporation technique. The solid-state analysis suggests that quercetin–nicotinamide cocrystals are a new phase, and interactions of the intermolecular hydrogen bonds exist between quercetin and nicotinamide in quercetin–nicotinamide cocrystals. The dissolution of quercetin–nicotinamide cocrystals is found to be significantly improved in comparison to that of quercetin crystals. The pharmacokinetic experiment in rats affirms that quercetin–nicotinamide cocrystals improve the bioavailability of quercetin significantly. This study will mean that the drug cocrystal technology will be an available solid form to improve the dissolution and oral bioavailability of insoluble medicines and to expand the clinical applications of quercetin.

## Conflicts of interest

There are no conflicts to declare.

## References

- H. P. Hoensch and R. Oertel, The value of flavonoids for the human nutrition: short review and perspectives, *Clin. Nutr. Exp.*, 2015, **3**, 8–14.
- D. Aune, E. Giovannucci, P. Boffetta, L. T. Fadnes, N. Keum, T. Norat, *et al.*, Fruit and vegetable intake and the risk of cardiovascular disease, total cancer and all-cause mortality—a systematic review and dose-response meta-analysis of prospective studies, *Int. J. Epidemiol.*, 2017, **46**(3), 1029–1056.
- A. W. Boots, G. R. Haenen and A. Bast, Health effects of quercetin: from antioxidant to nutraceutical, *Eur. J. Pharmacol.*, 2008, **585**, 325–337.
- M. Russo, C. Spagnuolo, I. Tedesco, S. Bilotto and G. L. Russo, The flavonoid quercetin in disease prevention and therapy: facts and fancies, *Biochem. Pharmacol.*, 2012, **83**, 6–15.
- S. Egert, S. Wolfram, A. Bosy-Westphal, C. Boesch-Saadatmandi, A. E. Wagner, J. Frank, G. Rimbach and M. J. Mueller, Daily quercetin supplementation dose-dependently increases plasma quercetin concentrations in healthy humans, *J. Nutr.*, 2008, **138**, 1615–1621.
- D. D. Hou, W. Zhang, Y. L. Gao, Y. Z. Sun, H. X. Wang, R. Q. Qi, H. D. Chen and X. H. Gao, Anti-inflammatory effects of quercetin in a mouse model of MC903-induced atopic dermatitis, *Int. Immunopharmacol.*, 2019, **74**, 105676.
- A. Murakami, H. Ashida and J. Terao, Multitargeted cancer prevention by quercetin, *Cancer Lett.*, 2008, **269**, 315–325.
- Y. Guo and R. S. Brun, Endogenous and exogenous mediators of quercetin bioavailability, *J. Nutr. Biochem.*, 2015, **26**, 201–210.
- V. Natarajan, N. Krithica, B. Madhan and K. Sehgal, Formulation and evaluation of quercetin polycaprolactone microspheres for the treatment of rheumatoid arthritis, *J. Pharm. Sci.*, 2011, **1**, 195–205.
- E. U. Graefe, H. Derendorf and M. Veit, Pharmacokinetics and bioavailability of the flavonol quercetin in humans, *Int. J. Clin. Pharmacol. Therapeut.*, 1999, **37**, 219–233.
- E. Sanchez-Rexach, J. Iturri, J. Fernandez, E. Meaurio, J. L. Toca-Herrera and J. R. Sarasua, Novel biodegradable and non-fouling systems for controlled-release based on poly( $\epsilon$ -caprolactone)/Quercetin blends and biomimetic bacterial S-layer coatings, *RSC Adv.*, 2019, **9**, 24154–24163.
- E. S. Kim, D. Y. Kim, J. S. Lee and H. G. Lee, Mucoadhesive Chitosan-Gum Arabic Nanoparticles Enhance the Absorption and Antioxidant Activity of Quercetin in the Intestinal Cellular Environment, *J. Agric. Food Chem.*, 2019, **67**, 8609–8616.
- G. Kuminek, F. Cao, A. Bahia de Oliveira da Rocha, S. Gonçalves Cardoso and N. Rodríguez-Hornedo, Cocrystals to facilitate delivery of poorly soluble compounds beyond-rule-of-5, *Adv. Drug Delivery Rev.*, 2016, **101**, 143–166.
- N. Shan and M. J. Zaworotko, The role of cocrystals in pharmaceutical science, *Drug Discovery Today*, 2008, **13**, 440–446.
- B. Sarma, J. Chen, H. Y. Hsi and A. S. Myerson, Solid forms of pharmaceuticals: polymorphs, salts and cocrystals, *Korean J. Chem. Eng.*, 2011, **28**, 315–322.
- M. Karimi-Jafari, L. Padrela, G. M. Walker and D. M. Croker, Creating cocrystals: a review of pharmaceutical cocrystal preparation routes and applications, *Cryst. Growth Des.*, 2018, **18**, 6370–6387.
- N. K. Duggirala, M. L. Perry, O. Almarsson and M. J. Zaworotko, Pharmaceutical cocrystals: along the path to improved medicines, *Chem. Commun.*, 2016, **52**(4), 640–655.



- 18 S. J. Bethune, N. Schultheiss and J. O. Henck, Improving the poor aqueous solubility of nutraceutical compound pterostilbene through cocrystal formation, *Cryst. Growth Des.*, 2011, **11**(7), 2817–2823.
- 19 Z. Li and A. J. Matzger, Influence of coformer stoichiometric ratio on pharmaceutical cocrystal dissolution: three cocrystals of carbamazepine/4-aminobenzoic acid, *Mol. Pharm.*, 2016, **13**, 990–995.
- 20 A. J. Smith, P. Kavuru, L. Wojtas, M. J. Zaworotko and R. Douglas Shytle, Cocrystals of quercetin with improved solubility and oral bioavailability, *Mol. Pharm.*, 2011, **8**, 1867–1876.
- 21 A. Heinz, K. C. Gordon, C. M. McGoverin, T. Rades and C. J. Strachan, Understanding the solid-state forms of fenofibrate-A spectroscopic and computational study, *Eur. J. Pharm. Biopharm.*, 2009, **71**, 100–108.
- 22 M. Fujimori, K. Kadota, K. Shimono, Y. Shirakawa, H. Sato and Y. Tozuka, Enhanced solubility of quercetin by forming composite particles with transglycosylated materials, *J. Food Eng.*, 2015, **149**, 248–254.

